



ELSEVIER

Journal of Computational and Applied Mathematics 143 (2002) 127–139

JOURNAL OF
COMPUTATIONAL AND
APPLIED MATHEMATICS

www.elsevier.com/locate/cam

A note on stability of pseudospectral methods for wave propagation

Z. Jackiewicz*, R.A. Renaut

Department of Mathematics, Arizona State University, Box 871 804, Tempe, Arizona, AZ 85287-1804, USA

Received 23 October 2000; received in revised form 25 April 2001

Abstract

In this paper we deal with the effects on stability of subtle differences in formulations of pseudospectral methods for solution of the acoustic wave equation. We suppose that spatial derivatives are approximated by Chebyshev pseudospectral discretizations. Through reformulation of the equations as first order hyperbolic systems any appropriate ordinary differential equation solver can be used to integrate in time. However, the resulting stability, and hence efficiency, properties of the numerical algorithms are drastically impacted by the manner in which the absorbing boundary conditions are incorporated. Specifically, mathematically equivalent well-posed approaches are not equivalent numerically. An analysis of the spectrum of the resultant system operator predicts these properties. © 2002 Elsevier Science B.V. All rights reserved.

MSC: 65M05; 65M10; 35L05

Keywords: Pseudospectral Chebyshev method; Absorbing boundary conditions; Hyperbolic systems; Wave equation; Runge–Kutta methods; Eigenvalue stability

1. Introduction

In this paper we propose and analyse a pseudospectral solution of the acoustic wave equation with absorbing boundary conditions (ABCs) for the first order hyperbolic system formulation of the problem. In [17,16] stability restrictions were determined through an analysis of the spectrum of the semi-discrete problem. This appeared to contradict a study of Driscoll and Trefethen [6] in which the one-dimensional (1D) acoustic wave propagation with one Dirichlet boundary was determined to have a non-normal operator. Their investigation was based on the conversion of the second order PDE to a hyperbolic system of first order PDEs. Here we perform the equivalent reformulation but with absorbing boundary conditions at all boundaries, for both the 1D and two-dimensional (2D)

* Corresponding author.

E-mail addresses: jackiewi@math.la.asu.edu (Z. Jackiewicz), renaut@asu.edu (R.A. Renaut).

case. In this situation the operators are near normal and an analysis of the spectrum does predict the stability properties.

In Section 2 we illustrate via the 1D problem that there are several possible algebraic possibilities for the inclusion of the continuous form of the ABCs in the hyperbolic system. Analyses of the spectra and pseudospectra of the underlying system operators successfully predict their stability properties. In particular, while all formulations are mathematically equivalent they do not all lead to stable numerical formulations. The situation is similar for the 2D problem studied in Section 3. But the spectrum of the underlying system operators predicts not only which formulations are stable but also those for which the boundary conditions are overprescribed, and hence are not well-posed. The resulting stable formulation offers not only improved efficiency compared to the second order formulation discussed in [17,16], but also greater flexibility for improvement of the overall accuracy because integration in time may be accomplished by any appropriate ordinary differential equation (ODE) solver.

2. 1D Acoustic wave propagation

To illustrate the impact that the algorithm has on stability we consider first the 1D wave equation

$$\begin{aligned} u_{tt} &= c^2 u_{xx}, & -\infty < x < \infty, & t > 0, \\ u(x, 0) &= f(x), & -\infty < x < \infty, \\ u_t(x, 0) &= 0, & -\infty < x < \infty. \end{aligned} \tag{2.1}$$

The solution $u(x, t) = \frac{1}{2}(f(x - ct) + f(x + ct))$ consists of two waves travelling in opposite directions with speed c .

We suppose that the numerical solution is only required on the restricted domain $\{x: 0 < x < 1\}$. This is achievable in the 1D case because the wave $\frac{1}{2}f(x - ct)$ travelling in the positive direction satisfies the characteristic equation $u_t + cu_x = 0$ at $x = 1$. Similarly, the wave $\frac{1}{2}f(x + ct)$ travelling in the negative direction satisfies $u_t - cu_x = 0$ at $x = 0$. Hence, the solution to (2.1) on the domain $\{x: 0 < x < 1\}$ can be found by augmenting (2.1) with the characteristic boundary conditions

$$\begin{aligned} u_t - cu_x &= 0, & x = 0, & t > 0, \\ u_t + cu_x &= 0, & x = 1, & t > 0. \end{aligned} \tag{2.2}$$

To increase the flexibility within the model, such that a standard ODE solver may be utilized for the time integration, we introduce the secondary variables $u_1 = u_t$ and $u_2 = u_x$. Then (2.1) and (2.2) are replaced by

$$u_{1,t} = c^2 u_{2,x}, \quad 0 < x < 1, \quad t > 0, \tag{2.3a}$$

$$u_{2,t} = u_{1,x}, \quad 0 < x < 1, \quad t > 0, \tag{2.3b}$$

$$u_1(x, 0) = 0, \quad 0 \leq x \leq 1, \tag{2.3c}$$

$$u_2(x, 0) = f_x(x), \quad 0 \leq x \leq 1, \tag{2.3d}$$

and

$$u_1 - cu_2 = 0, \quad x = 0, \quad t > 0, \tag{2.4a}$$

$$u_1 + cu_2 = 0, \quad x = 1, \quad t > 0. \tag{2.4b}$$

Note that (2.4a) and (2.4b) immediately prescribe values for u_1 in terms of u_2 , or u_2 in terms of u_1 , at the boundaries, and (2.3b) is just the consistency condition $u_{xt} = u_{tx}$.

In all cases first order spatial derivatives are approximated via the Chebyshev pseudospectral method collocated at the Chebyshev–Gauss–Lobatto points, numbered from left to right on the interval $[x_1, x_m] = [0, 1]$, see for example Canuto et al. [4]. Applied to (2.3) this yields the compact system

$$\begin{aligned} U_t &= AU, \quad t > 0, \\ U(0) &= [0^T, (DF)^T]^T, \end{aligned} \tag{2.5}$$

where

$$\begin{aligned} A &= \left[\begin{array}{c|c} 0 & c^2 D \\ \hline D & 0 \end{array} \right], \\ F^T &= [f(x_1), \dots, f(x_m)], \end{aligned}$$

and

$$U^T = [u_1(x_1, t), \dots, u_1(x_m, t), u_2(x_1, t), \dots, u_2(x_m, t)].$$

Here D denotes the pseudospectral first order differentiation matrix of size $m \times m$, with columns denoted by d_k , $1 \leq k \leq m$, and can be efficiently computed by the algorithm described in [7,8], or [20], see also [1].

To incorporate the characteristic boundary conditions (2.4a) and (2.4b) in (2.5) we choose $u_2(x_1) = u_1(x_1)/c$ and $u_2(x_m) = -u_1(x_m)/c$, respectively. In this case we obtain the new system

$$U_{1,t} = A_1 U_1, \quad t > 0, \tag{2.6}$$

where

$$A_1 = \left[\begin{array}{c|c} cd_1 \ 0_{m \times (m-2)} & -cd_m \ c^2 D(1 : m, 2 : m-1) \\ \hline D(2 : m-1, 1 : m) & 0_{(m-2) \times (m-2)} \end{array} \right],$$

and

$$U_1^T = [u_1(x_1), \dots, u_1(x_m), u_2(x_2), \dots, u_2(x_{m-1})].$$

Alternatively, elimination of $u_1(x_1)$ and $u_1(x_m)$ via $u_1(x_1) = cu_2(x_1)$ and $u_1(x_m) = -cu_2(x_m)$, respectively, yields

$$U_{2,t} = A_2 U_2, \quad t > 0, \tag{2.7}$$

where

$$A_2 = \left[\begin{array}{c|c} 0_{(m-2) \times (m-2)} & c^2 D(2 : m-1, 1 : m) \\ \hline D(1 : m, 2 : m-1) & cd_1 \ 0_{m \times (m-2)} \ -cd_m \end{array} \right],$$

and

$$U_2^T = [u_1(x_2), \dots, u_1(x_{m-1}), u_2(x_1), \dots, u_2(x_m)].$$

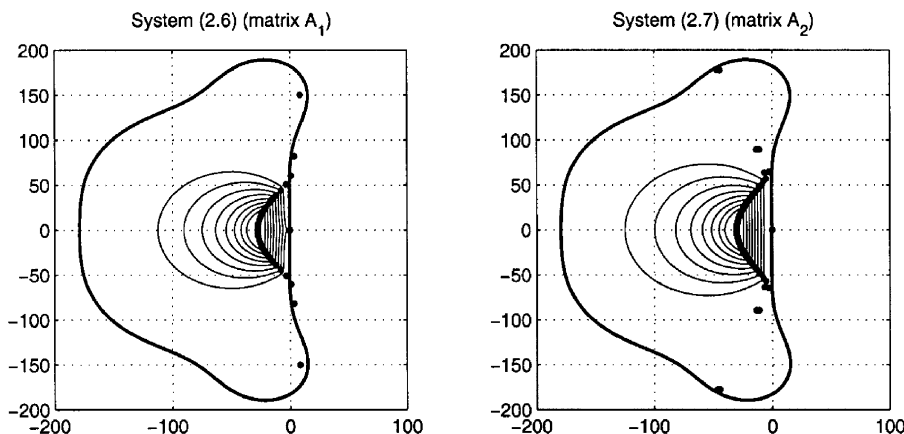


Fig. 1. Spectra and ε -pseudospectra of matrices A_1 and A_2 for $m = 32$.

These systems, which are mathematically equivalent, apply the boundary conditions implicitly and are equivalent to the choices $u_{tt} = c^2 u_{xx}, 0 \leq x \leq 1$ with $u_{tx} = u_{xt}, 0 < x < 1$ for matrix A_1 , and $u_{tt} = c^2 u_{xx}, 0 < x < 1$ with $u_{tx} = u_{xt}, 0 \leq x \leq 1$ for matrix A_2 . They also can be interpreted as limiting cases of a penalty method in which the penalties are Dirac delta functions at the boundaries. This point is further discussed in [17]. In particular, when the penalty terms are not taken as Dirac delta functions the system matrices are modified accordingly, [10]. Moreover, alternative choices for the incorporation of the boundary conditions lead to yet different system matrices. For example, the boundary conditions could be incorporated by elimination of $u_2(x_1)$ and $u_1(x_m)$, or $u_2(x_m)$ and $u_1(x_1)$ in the partial differential equation. We will illustrate for systems with matrices A_1 and A_2 that such subtle changes significantly impact the stability properties of the method.

The semi-discrete systems with matrices A_1 and A_2 , continuous in time, can be integrated by any appropriate ordinary differential equation (ODE) solver. Because our emphasis is on the behavior due to the spatial discretization we chose a standard scheme; the explicit Runge–Kutta method of order four (RK4), compare [3,13].

To assure stable integration, in the sense of “eigenvalue stability”, for a given spatial discretization with system matrix A we have to choose the stepsize Δt of the method in such a way that the spectrum $\sigma(A)$ scaled by Δt is contained in the region of absolute stability \mathcal{A} of the method [19]. This verification of stability assumes that A is normal or, in some sense, close to normal. Otherwise it is necessary to work with the ε -pseudospectra where the ε -pseudospectrum of A , for each $\varepsilon \geq 0$, is defined by $\Lambda_\varepsilon(A) = \{z \in \mathbf{C}: \|(zI - A)^{-1}\| \geq \varepsilon^{-1}\}$; see Reddy and Trefethen [18].

The spectra and ε -pseudospectra of A_1 and A_2 for $m = 32$ and $\varepsilon = 10^{-k}, k = 2, 3, \dots, 9$, and the scaled region of absolute stability of the RK4 method are plotted in Fig. 1. The illustrated eigenvalues of A_1 are relatively insensitive to perturbations. Matrix A_1 also has an outlier real eigenvalue of multiplicity two at -906.7 which is insensitive to perturbation. Some of the eigenvalues of A_1 are for $m \geq 16$, however, in the right-half plane. While this need not violate the eigenvalue stability of the numerical method if \mathcal{A} extends into the right half plane, Δt must be taken small enough that the growth of the spurious solutions associated with these eigenvalues is maintained to be insignificant as compared to the size of the physical solution, which does not grow in time. On the other hand,

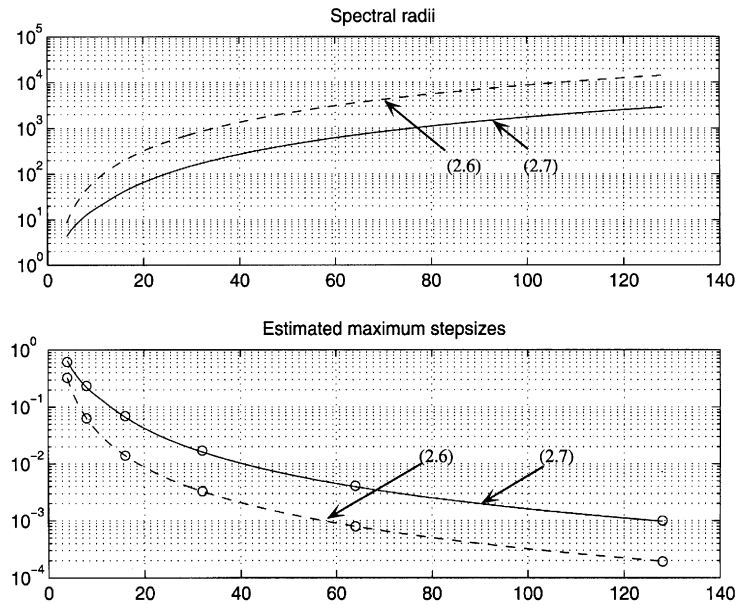


Fig. 2. Spectral radii and estimated maximum timesteps, plotted on a \log_{10} scale against subdimension size m , for systems (2.6) (dashed lines) and (2.7) (solid lines), respectively.

while eigenvalues of A_2 are somewhat more sensitive, there are no eigenvalues in the right half plane, and the complex outliers determine the stability limits on timestep Δt for time integration.

We have plotted in Fig. 2, using a log scale for the y -axes, the spectral radii $\rho(A_1)$ (dashed line) and $\rho(A_2)$ (solid line) of the matrices A_1 and A_2 as functions of the subdimension m , and the estimated maximum stepsizes $\Delta t_{1,\max}$ (dashed line) and $\Delta t_{2,\max}$ (solid line) which should assure stable integration. These stepsizes are computed by the formula

$$\Delta t_{i,\max} = \frac{2.78}{\rho(A_i)}, \tag{2.8}$$

$i = 1, 2$. This formula assumes that the last point of entry of the scaled spectra $\Delta t\sigma(A_1)$ and $\Delta t\sigma(A_2)$ into the region of absolute stability of the RK4 method is at the point on the negative real axis approximately equal to -2.78 . This point is the left end of the interval of absolute stability for method. While this will provide a reasonable estimate for matrix A_1 because the eigenvalue of maximum absolute value is real, the eigenvalue of maximum absolute value for A_2 is not real and Δt_{\max} will be underestimated. A more accurate calculation using the extent of the stability region in the direction of the eigenvalue of largest absolute value gives the values in Table 1. We observe that, for $m \geq 16$, the maximum stepsize for stable integration of system with matrix A_2 is theoretically larger by a factor of about five than that for system with matrix A_1 . Moreover, the eigenvalues of A_1 with positive real point are well within \mathcal{A} when multiplied by Δt_{\max} .

Numerical experiments were carried out to verify the estimates provided in Table 1 and to illustrate the effectiveness of the stability analysis. The numerical approximation to $u(x, t)$, denoted by $u_{\Delta t}$, is not given immediately from the time-stepped solution to the semi-discrete systems. Rather,

Table 1
Maximum stable timestep for systems with matrices A_1 and A_2 , in conjunction with RK4

m	$\Delta t_{1,\max}$ for A_1	$\Delta t_{2,\max}$ for A_2	$\frac{\Delta t_{2,\max}}{\Delta t_{1,\max}}$
4	0.325e + 00	0.615e + 00	1.89
8	0.633e - 01	0.235e + 00	3.71
16	0.139e - 01	0.690e - 01	4.96
32	0.330e - 02	0.170e - 01	5.15
64	0.791e - 03	0.410e - 02	5.18
128	0.192e - 03	0.101e - 02	5.26

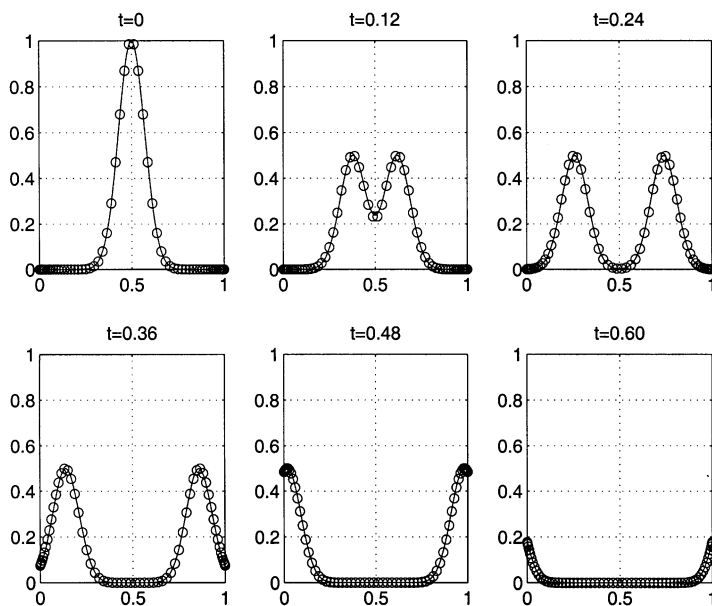


Fig. 3. Exact and numerical solution for the system with matrix A_2 .

approximations $u_{1,\Delta t}$ and $u_{2,\Delta t}$ to u_1 and u_2 must be computed. To obtain $u_{\Delta t}$ the fourth order interpolant in time

$$u_{\Delta t}(x_i, t_{v+3}) = u_{\Delta t}(x_i, t_v) + \Delta t(\beta_0 u_{1,\Delta t}(x_i, t_v) + \beta_1 u_{1,\Delta t}(x_i, t_{v+1}) + \beta_2 u_{1,\Delta t}(x_i, t_{v+2}) + \beta_3 u_{1,\Delta t}(x_i, t_{v+3})), \tag{2.9}$$

$i = 1, 2, \dots, m$, where

$$\beta_0 = -\frac{51}{8}, \quad \beta_1 = \frac{171}{8}, \quad \beta_2 = -\frac{153}{8}, \quad \beta_3 = \frac{57}{8}, \tag{2.10}$$

was used.

In Fig. 3 the numerical results are presented for system matrix A_2 with $c=1$, $m=64$, and $\Delta t=0.004$ for the time interval $0 < t < 0.6$. The initial function f was defined as a pulse of

the form

$$f(x) = \exp(-a(x - x_0)^2),$$

with $a = 100$ and $x_0 = 0.5$. The true solution u is plotted by a solid line and numerical approximations by the points marked by the symbol ‘o’. We observe that the boundaries are transparent, as expected, for waves travelling in both directions with speed $c = 1$. Similar behaviour was observed for nonsmooth initial functions.

Our analysis demonstrates that, despite the mathematical equivalence of the continuous partial differential equations with system matrices A_1 and A_2 , the resulting numerical algorithms are different. The only difference in formulation is that for A_2 the partial differential equation is explicitly applied on the interior domain, and only implicitly applied at the boundaries, whereas for A_1 it is also explicit at the boundaries. However, the latter operator does not permit the integration of the system over arbitrarily large time intervals. Numerical results confirm that, for the given time interval of integration, convergence is not achieved when $m = 128$. Integration over larger time intervals would also show non-convergence for smaller m .

3. 2D Acoustic wave propagation

We now extend the discussion of Section 2 to the numerical solution of the 2D problem:

$$\begin{aligned} u_{tt} &= c^2(u_{xx} + u_{yy}), & -\infty < x, y < \infty, & t > 0, \\ u(x, y, 0) &= f(x, y), & -\infty < x, y < \infty, & \\ u_t(x, y, 0) &= 0, & -\infty < x, y < \infty, & \end{aligned} \tag{3.1}$$

on the restricted numerical domain $\{(x, y) : 0 < x, y < 1\}$. To extend the approach in Section 2 we restrict attention, as in [17], to the use of the characteristic equations for absorption of waves at the boundaries,

$$\begin{aligned} u_t - cu_x &= 0, & x = 0, & 0 \leq y \leq 1, \\ u_t + cu_x &= 0, & x = 1, & 0 \leq y \leq 1, \\ u_t - cu_y &= 0, & y = 0, & 0 \leq x \leq 1, \\ u_t + cu_y &= 0, & y = 1, & 0 \leq x \leq 1. \end{aligned} \tag{3.2}$$

The extension to higher order one-way wave equations, [5,9,11,12,14–17], or the PML approach of Berenger [2], used in conjunction with pseudospectral approximations, is nontrivial, and will be the subject of future work.

We reformulate (3.1) as a hyperbolic system of first order by introducing the standard notation $u_1 = u_t$, $u_2 = u_x$, and $u_3 = u_y$. Then (3.1) can be rewritten as

$$\begin{aligned} u_{1,t} &= c^2(u_{2,x} + u_{3,y}), & 0 \leq x, y \leq 1, & t > 0, \\ u_{2,t} &= u_{1,x}, & 0 \leq x, y \leq 1, & \end{aligned}$$

$$\begin{aligned}
 u_{3,t} &= u_{1,y}, & 0 \leq x, y \leq 1, \\
 u_1(x, y, 0) &= 0, & 0 \leq x, y \leq 1, \\
 u_2(x, y, 0) &= f_x(x, y), & 0 \leq x, y \leq 1, \\
 u_3(x, y, 0) &= f_y(x, y), & 0 \leq x, y \leq 1,
 \end{aligned} \tag{3.3}$$

and the characteristic equations become

$$\begin{aligned}
 u_1 - cu_2 &= 0, & x=0, & 0 \leq y \leq 1, \\
 u_1 + cu_2 &= 0, & x=1, & 0 \leq y \leq 1, \\
 u_1 - cu_3 &= 0, & y=0, & 0 \leq x \leq 1, \\
 u_1 + cu_3 &= 0, & y=1, & 0 \leq x \leq 1.
 \end{aligned} \tag{3.4}$$

Spatial derivatives in x and y directions are obtained analogously as for the x derivatives in Section 2 using the Chebyshev–Gauss–Lobatto points in each direction. The resulting semi-discrete formulation can be expressed compactly as a matrix vector system

$$\begin{aligned}
 U_t &= AU, \quad t > 0, \\
 U(0) &= [0^T, ((I_m \otimes D)F)^T, ((D \otimes I_m)F)^T]^T
 \end{aligned} \tag{3.5}$$

where

$$A = \left[\begin{array}{c|c|c} 0 & c^2(I_m \otimes D) & c^2(D \otimes I_m) \\ \hline I_m \otimes D & 0 & 0 \\ \hline D \otimes I_m & 0 & 0 \end{array} \right], \quad U = \begin{bmatrix} u_1 \\ u_2 \\ u_3 \end{bmatrix},$$

$$\begin{aligned}
 u_i(t) &= [u_i(x_1, y_1, t), \dots, u_i(x_m, y_1, t), \dots, u_i(x_1, y_m, t), \dots, u_i(x_m, y_m, t)]^T, \quad i = 1, 2, 3, \text{ and} \\
 F &= [f(x_1, y_1), \dots, f(x_m, y_1), \dots, f(x_1, y_m), \dots, f(x_m, y_m)]^T.
 \end{aligned}$$

Here ‘ \otimes ’ is the tensor product and I_m stands for the identity matrix of dimension m .

Again the characteristic equations can be incorporated into the partial differential equation in many ways. Eliminating u_2 and u_3 in (3.5) for $0 \leq y \leq 1$ and $0 \leq x \leq 1$, respectively, using u_1 from (3.4), gives a formulation equivalent to the 1D system with matrix A_1 ,

$$U_{1,t} = A_1 U_1. \tag{3.6}$$

Alternatively, eliminating u_1 in the first subsystem of (3.5) using equations (3.4) gives a system equivalent to the 1D case with matrix A_2 ,

$$U_{2,t} = A_2 U_2. \tag{3.7}$$

A third option, which is also well-posed, is obtained by using Eqs. (3.4) to eliminate u_2 and u_3 from the second and third subsystems in (3.5)

$$U_{3,t} = A_3 U_3. \tag{3.8}$$

Here U_1, U_2 and U_3 are the appropriate modifications of U after elimination of the stated variables.

We have repeated the analysis of Section 2 for systems with matrices A_1, A_2 , and A_3 . In Fig. 4 we have plotted spectra and ε -pseudospectra of matrices A_1, A_2 , and A_3 for $m = 16$ and $\varepsilon = 10^{-k}$, $k =$

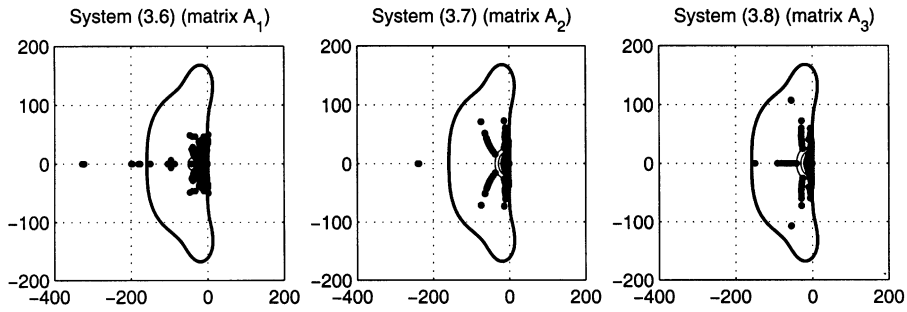


Fig. 4. Spectra and ε -pseudospectra of matrices A_1, A_2, A_3 for $m = 16$.

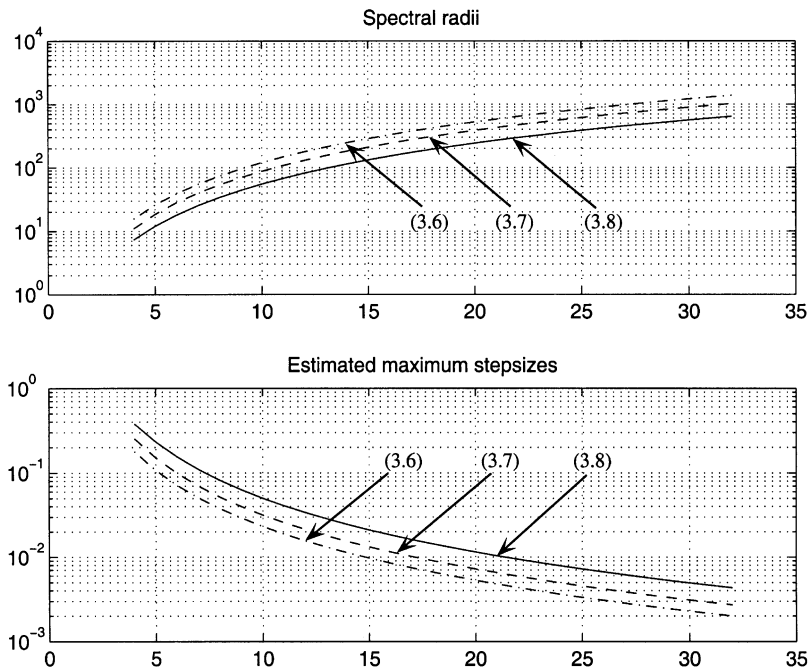


Fig. 5. Spectral radii and estimated maximum timesteps, plotted on a \log_{10} scale against subdimension size m , for systems with matrices A_1 (dashdotted lines), A_2 (dashed lines), and A_3 (solid lines), respectively.

2, 3, ..., 9, and the scaled region of absolute stability for RK4. As before the outlier eigenvalues of matrices A_1, A_2 , and A_3 are insensitive to small perturbations, and thus we conclude that eigenvalue stability is sufficient for these systems.

Spectral radii of matrices A_1, A_2 and A_3 , and estimated maximum time-steps for stable integration in time using RK4 as computed by the formula (2.8), are plotted on a log scale in Fig. 5, where we have used dashdotted lines for properties of A_1 , dashed lines for properties of A_2 , and solid lines for properties of A_3 . The estimate for the maximum time-step is somewhat more accurate than in the 1D case because $\rho(A_2)$ and $\rho(A_3)$ coincide with the largest in modulus negative real eigenvalue.

Table 2
 Maximum timesteps for integration of systems with matrices A_1 , A_2 and A_3 using RK4

m	$\Delta t_{1,\max}$ for A_1	$\Delta t_{2,\max}$ for A_2	$\Delta t_{3,\max}$ for A_3	$\frac{\Delta t_{3,\max}}{\Delta t_{2,\max}}$	$\frac{\Delta t_{3,\max}}{\Delta t_{1,\max}}$
4	0.1790	0.2540	0.3790	1.49	2.12
8	0.0377	0.0518	0.0818	1.58	2.17
16	0.0850	0.0115	0.0184	1.60	2.16
32	0.0020	0.0027	0.0043	1.59	2.15

Again for $m = 16$ and 32 , matrix A_1 has some eigenvalues with positive real part, which dictates that the time interval for integration is limited to that for which the growth of the spurious solutions is maintained as insignificant. We see also that the system with matrix A_3 theoretically allows stepsizes larger by a factor of about 1.5 than that with A_2 .

Numerical verification was carried out following the procedure described in Section 2. The initial function was defined as

$$f(x, y) = \exp(-a((x - x_0)^2 + (y - y_0)^2)),$$

which is a pulse centered at the point (x_0, y_0) . These problems were solved for $c = 1$, $a = 100$, $m = 32$, $\Delta t = 0.004$ on the time interval $0 < t < 0.8$. The results of numerical simulations were then interpolated to the uniform grid $\{(\bar{x}_i, \bar{y}_j) : i, j = 1, 2, \dots, \bar{m}\}$ consisting of $\bar{m} = 2m = 64$ points in each space dimension as described in Appendix A. These experiments confirmed the validity of the estimates of $\Delta t_{i,\max}$ presented in Table 2.

The results of numerical simulations with system matrix A_3 with a pulse centered at $(x_0, y_0) = (0.5, 0.5)$ are presented in Fig. 6 and with a pulse centered at $(x_0, y_0) = (0.75, 0.25)$ in Fig. 7. It is apparent that there is limited reflection at the artificial numerical boundaries. Better accuracy cannot be expected without imposing more sophisticated absorbing boundary conditions. This will be the subject of future work.

4. Concluding remarks

The analysis presented in Sections 2 and 3 demonstrates the subtleties involved in utilizing pseudospectral methods for solution of Eqs. (2.1) and (3.1) on artificially-bounded domains. In contrast to the approach in [16,17], Eqs. (2.1) and (3.1) are recast as hyperbolic systems of first order, with a goal to provide greater flexibility in time-stepping. The appropriate formulation is not immediately obvious from physical considerations, and an analysis of the spectrum and pseudospectrum of the underlying system matrix is required to determine both the stability properties and the limits on the allowable timesteps for stability. In particular, while alternative formulations may be stable, the size of stable timestep depends directly on the specific formulation.

A more detailed study to determine the trade-offs between the spatial and temporal accuracy, and required memory resources of the first order formulation, as compared to the second order formulation, will be presented in a future report.

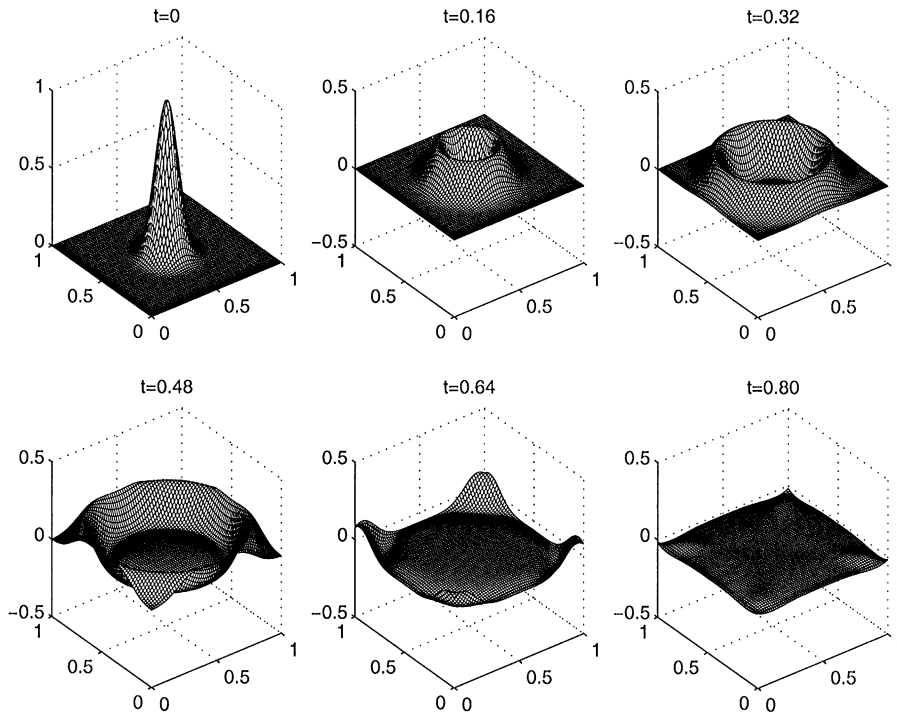


Fig. 6. Numerical results for the formulation with matrix A_3 for initial pulse centered at $(x_0, y_0) = (0.5, 0.5)$.

Acknowledgements

The authors wish to express their gratitude to Professor L.N. Trefethen for useful comments and for providing us with his program for plotting pseudospectra. This work was supported by the National Science Foundation under grants DMS-9971164 (Z. Jackiewicz) and DMS-9402943 (R.A. Renaut).

Appendix A.

While a lower order interpolant may be used, as for example, by use of Matlab’s command `interp2`, see Program 20 in [20], to obtain a graphical representation of the solution, this may obscure the reflections from the numerical boundaries. Here the global polynomial interpolant defined by the Chebyshev expansion is used to interpolate the results on the Chebyshev grid to a finer uniform grid $\{(\bar{x}_i, \bar{y}_j) : i, j, = 1, 2, \dots, \bar{m}\}$, where $\bar{m} = 2m$, [4]. Although this can be implemented using the fast Fourier transform, we illustrate this approach using matrix notation.

To compute the required approximations $u_{\Delta t}(x, y, t)$ to the solution $u(x, y, t)$ we use the Chebyshev expansion for $u_{\Delta t}$ in terms of the expansion coefficients $q_{kl}(t)$

$$u_{\Delta t}(x, y, t) = \sum_{k=1}^m \sum_{l=1}^m q_{kl}(t) T_{k-1}(x) T_{l-1}(y), \tag{A.1}$$

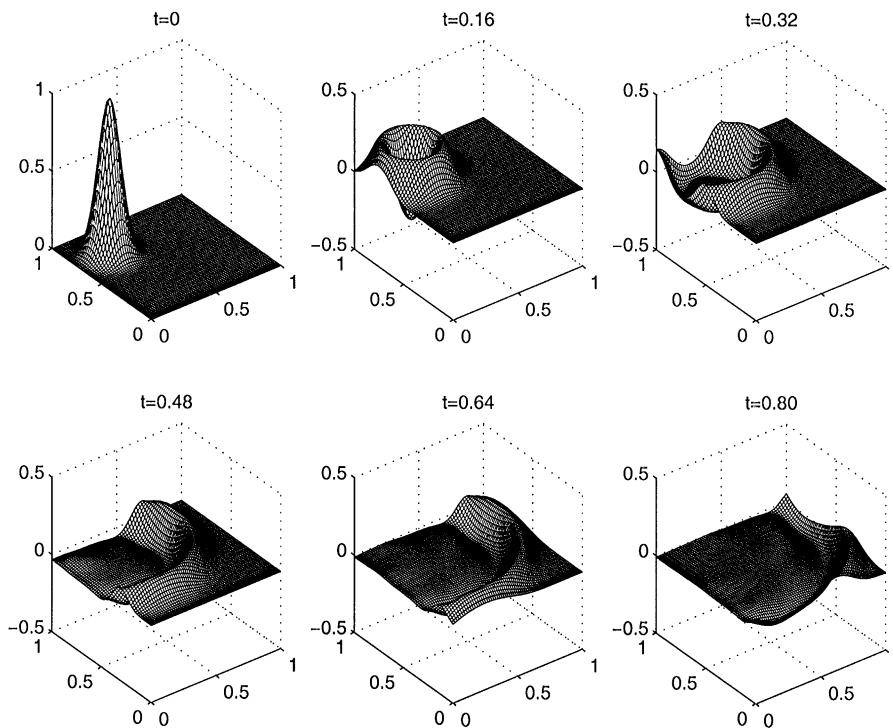


Fig. 7. Numerical results for the formulation with matrix A_3 for an initial pulse centered at $(x_0, y_0) = (0.75, 0.25)$.

where $T_l(x) = \cos(l \cos^{-1}(2x - 1))$, $x \in [0, 1]$ is the Chebyshev polynomial of degree l defined on the interval $[0, 1]$. The expansion coefficients $q_{kl}(t)$, $k, l = 1, 2, \dots, m$ can be computed from the interpolation property

$$u_{\Delta t}(x_i, y_j, t) = \sum_{k=1}^m \sum_{l=1}^m q_{kl}(t) T_{k-1}(x_i) T_{l-1}(y_j), \quad i, j = 1, 2, \dots, m, \tag{A.2}$$

where $u_{\Delta t}(x_i, y_j, t)$ are the numerical approximations to $u(x_i, y_j, t)$ at the Chebyshev–Gauss–Lobatto points $\{(x_i, y_j) : i, j = 1, 2, \dots, m\}$, [4]. Equivalently,

$$u_{\Delta t} = R^T Q R,$$

where $u_{\Delta t} = [u_{\Delta t}(x_i, y_j, t)]_{i,j=1}^m$, $Q = Q(t)$ with entries q_{kl} , and $R = [r_{ij}]_{i,j=1}^m$ is given by

$$r_{ij} = T_{i-1}(x_j) = \cos \frac{\pi(i-1)(m-j)}{m-1}, \quad i, j = 1, 2, \dots, m.$$

The inverse R^{-1} of the matrix R is known explicitly, and is given by

$$(R^{-1})_{ij} = \frac{2}{(m-1)\bar{c}_j \bar{c}_i} \cos \frac{\pi(i-1)(m-j)}{m-1}, \quad i, j = 1, 2, \dots, m$$

where

$$\bar{c}_j = \begin{cases} 2 & j = 1, m, \\ 1 & 2 \leq j \leq m - 1, \end{cases}$$

compare [4]. Thus, from (A.2), $Q = (R^{-1})^T u_{\Delta t} R^{-1}$ and (A.1) can be evaluated for any set of points. For example, for the uniform grid we obtain the approximation $\bar{u}_{\Delta t} = \bar{R}^T Q \bar{R}$, $\bar{R} = [\bar{r}_{ij}]_{i=1, j=1}^{m, \bar{m}}$, $\bar{r}_{ij} = T_{i-1}(\bar{x}_j) = \cos((i-1)\cos^{-1}(2\bar{x}_j - 1))$, $i = 1, 2, \dots, m$, $j = 1, 2, \dots, \bar{m}$.

References

- [1] R. Baltensperger, J.P. Berrut, The errors in calculating the pseudospectral differentiation matrices for Chebyshev–Gauss–Lobatto points, *Comput. Math. Appl.* 68 (1999) 1109–1120.
- [2] J.P. Berenger, A perfectly matched layer for absorption of electromagnetic waves, *J. Comput. Phys.* 114 (1994) 185–200.
- [3] J.C. Butcher, *The Numerical Analysis of Ordinary Differential Equations. Runge–Kutta and General Linear Methods*, Wiley, Chichester, New York, 1987.
- [4] C. Canuto, M.Y. Hussaini, A. Quarteroni, T.A. Zang, *Spectral Methods in Fluid Dynamics*, Springer, New York, 1988.
- [5] R. Clayton, B. Engquist, Absorbing boundary conditions for acoustic and elastic wave equations, *Bull. Seismol. Soc. Am.* 67 (1977) 1524–1540.
- [6] T.A. Driscoll, L.N. Trefethen, Pseudospectra of the wave operator with an absorbing boundary, *J. Comp. Appl. Math.* 69 (1996) 125–142.
- [7] B. Fornberg, Generation of finite difference formulas on arbitrarily spaced grids, *Math. Comp.* 51 (1988) 699–706.
- [8] B. Fornberg, *A Practical Guide to Pseudospectral Methods*, Cambridge University Press, Cambridge, 1996.
- [9] L. Halpern, L.N. Trefethen, Wide-angle one-way wave equations, *J. Acoust. Soc. Am.* 84 (1988) 1397–1404.
- [10] J.S. Hesthaven, D. Gottlieb, A stable penalty method for the compressible Navier Stokes equations. I. Open boundary conditions, *SIAM J. Sci. Comput.* 17 (1996) 579–612.
- [11] R.L. Higdon, Absorbing boundary conditions for difference approximations to the multi-dimensional wave equation, *Math. Comp.* 47 (1986) 437–459.
- [12] R.L. Higdon, Numerical absorbing boundary conditions for the wave equation, *Math. Comp.* 49 (1987) 65–90.
- [13] J.D. Lambert, *Computational Methods in Ordinary Differential Equations*, Wiley, Chichester, New York, 1973.
- [14] E.L. Lindman, Free Space Boundary Conditions for the Time Respondent Wave Equation, *J. Comput. Phys.* 18 (1975) 66–78.
- [15] R.A. Renaut, Absorbing boundary conditions, difference operators, and stability, *J. Comput. Phys.* 102 (1992) 236–251.
- [16] R.A. Renaut, Stability of Chebyshev pseudospectral solution of the wave equation with absorbing boundaries, *J. Comput. Appl. Math.* 87 (1997) 243–259.
- [17] R.A. Renaut, J. Fröhlich, A pseudospectral Chebyshev method for the 2-D wave equation with domain stretching and absorbing boundary conditions, *J. Comput. Phys.* 124 (1996) 324–336.
- [18] S.C. Reddy, L.N. Trefethen, Lax-stability of fully discrete spectral methods via stability regions and pseudo-eigenvalues, *Comput. Meth. Appl. Mech. Eng.* 80 (1990) 147–164.
- [19] L.N. Trefethen, Lax-stability vs. eigenvalue stability of spectral methods, in: K.W. Morton, M.J. Baines (Eds.), *Numerical Methods for Fluid Dynamics III*, Clarendon Press, Oxford, 1988.
- [20] L.N. Trefethen, *Spectral Methods in Matlab*, Society for Industrial and Applied Mathematics, Philadelphia, 2000.